ORIGINAL ARTICLE

A detachable coating of cholesterol-anchored PEG improves tumor targeting of cell-penetrating peptide-modified liposomes

Jie Tang, Li Zhang, Han Fu, Qifang Kuang, Huile Gao, Zhirong Zhang, Qin He[*]

Key Laboratory of Drug Targeting and Drug Delivery Systems, Ministry of Education, West China School of Pharmacy, Sichuan University, Chengdu 610041, China

Abstract   Cell-penetrating peptides (CPPs) have been widely used to enhance the membrane transloca-tion of various carriers for many years, but the non-specificity of CPPs seriously limits their utility *in vivo*. In this study, cholesterol-anchored, reduction-sensitive PEG (first synthesized by our laboratory) was applied to develop a co-modified liposome with improved tumor targeting. Following optimization of the formulation, the *in vitro* and *in vivo* properties of the co-modified liposome were evaluated. The co-modified liposome had a much lower cellular uptake and tumor spheroid uptake, but a much higher tumor accumulation compared to CPP-modified liposome, indicating the non-specific penetration of CPPs could be attenuated by the outer PEG coating. With the addition of exogenous reducing agent, both the *in vitro* and *in vivo* cellular uptake was markedly increased, demonstrating that the reduction-sensitive PEG coating achieved a controllable detachment from the surface of liposomes and did not affect the penetrating abilities of CPPs. The present results demonstrate that the combination of cholestervsitive PEG and CPPs is an ideal alternative for the application of CPP-modified carriers *in vivo*.

*Corresponding author at: West China School of Pharmacy, Sichuan University, No. 17 Block 3 Southern Renmin Road, Chengdu, Sichuan 610041, China. Tel./fax: +86 28 85502532.
    E-mail address: qinhe@scu.edu.cn (Qin He).

Production and hosting by Elsevier

1. Introduction

Cancer is one of the world′s most deadly diseases and tumor-targeted drug delivery systems are currently an important approach for cancer treatment[1–3]. However, several barriers need to be overcome in order to achieve ideal therapeutic efficacy. Most critical is the penetration of cytoplasmic and organelle membranes by chemotherapeutic agents[4]. In many cases, cell-penetrating peptides (CPPs) have been successfully used to deliver a large variety of cargoes into individual cell organelles, resulting in dramatically improved therapeutic outcomes[5,6]. Furthermore, some CPPs promote lysosome escape[7] or nuclear targeting of various cargoes[8].

However, CPPs penetrate cells without selectivity and also bind plasma proteins easily, leading to recognition and clearance by the reticuloendothelial system (RES)[9]. The latter property of CPP-modified carriers accounts for their susceptibility to the so-called "kinetic barriers"[10], a significant obstacle for drug delivery[11]. Recently, smart stimuli-sensitive delivery systems have been designed to endow CPP-containing formulations with selective drug delivery and to increase circulation time *in vivo* without weakening cell penetration[12–14]. In these delivery systems, the function of CPPs can be selectively switched "on" and "off" by the outer stimuli-sensitive PEG[15]. So far, a variety of stimuli-sensitive PEG has been used in such delivery systems. Among these, the reduction-sensitive PEG (based on disulfide linkage) is easy to construct. The PEG detachment in this drug system can also be precisely controlled by exogenous reducing agent[16].

In our previous work, a cholesterol-anchored reduction-sensitive PEG was successfully synthesized for the first time[17]. In that study, we developed a multifunctional liposome (CL-R8-LP) incorporating two important properties. Octaarginines (R8, a representative CPP) were used to penetrate the cytoplasmic membrane barrier for liposomal drug delivery, and a detachable coating from a cholesterol-anchored reduction-sensitive PEG was applied to resist "kinetic barriers". Presently, we have optimized the formulation of CL-R8-LP by varying the concentrations of PEG and R8, and characterized the *in vitro* cellular uptake and tumor spheroid uptake of this formulation. *In vivo* and *ex vivo* tumor imaging has further verified the tumor-targeting ability of R8-modified liposomes containing the detachable PEG coating.

2. Materials and methods

2.1. Materials

Egg phosphatidylcholine (EPC) and 1,2-dioleoyl-*sn*-glycero-3-phosphoethanolamine-*N*-(carboxyfluorescein) (CFPE) were purchased from Avanti Polar Lipids, Inc. (Alabaster, USA). Cholesterol (CHO) and cysteine (Cys) were purchased from Chengdu Kelong Chemical Company (Chengdu, China). All the cholesterol anchored functional materials were synthesized by our laboratory according to a previously reported method[17], including the cholesterol anchored reduction-sensitive PEG (CHO-S-S-PEG$_{5000}$), R8 modified PEG (CHO-PEG$_{2000}$-R8) and non-cleavable PEG$_{2000}$ (CHO-mPEG$_{2000}$). Agarose LMP was purchased from Invitrogen (Carlsbad, CA). 1,1′-Dioctadecyl-3,3,3′,3′-tetramethylindodicarbocyanine 4-chlorobenzenesulfonate salt (DID) was obtained from Biotium (Hayward, CA). Other chemicals and reagents were of analytical grade.

Male BALB/c mice weighing 20–25 g were purchased from Experiment Animal Center of Sichuan University (China). All the animal experiments adhered to the principles of care and use of laboratory animals and were approved by the Experiment Animal Administrative Committee of Sichuan University.

2.2. Preparation of liposomes

Liposomes modified with different cholesterol anchored functional lipids were prepared by the lipid film hydration-ultrasound method[18]. Briefly, the basic composition was EPC/CHO=65:35, and the percentage of cholesterol decreased with the addition of various cholesterol anchored functional lipids. All the lipids were dissolved in chloroform and a lipid film was obtained after the solvent was evaporated by rotary evaporator at 37 °C for 15 min. The lipid film was then hydrated in PBS (pH 7.4) at 37 °C for 1 h, and further sonicated with a probe sonicator at 80 W for 75 s. To prepare CFPE-labeled and DID-loaded liposomes, CFPE and DID fluorescence probe were dissolved in chloroform at the beginning, following operations were the same as described above. The total lipid concentration of liposomes was at 3 mmol/L.

2.3. Characterization of liposomes

The size and zeta-potential of liposomes were detected by Malvern Zetasizer Nano ZS90 (Malvern Instruments Ltd., UK). Prior to measurement, 100 μL of the sample was diluted to 1 mL using the same buffer.

2.4. Cell culture

C26 cells were grown in RPMI-1640 medium (GIBCO) containing 10% FBS, 100 μg/mL streptomycin, and 100 U/mL penicillin. The cells were maintained at 37 °C in a humidified incubator with 5% CO$_2$.

2.5. Cellular uptake study

For the cellular uptake study, about 1×10^5 cells per well were seeded in 6-well plates and cultured for 24 h. The CFPE-labeled liposomes were added to the plates with a total lipid concentration of 0.3 mmol/L. After incubation in the absence or presence of Cys (10 mmol/L) which was used to provide a reducing environment for the cleavage of reduction-sensitive PEG for 4 h at 37 °C[16,19], the cells were washed three times with cold PBS (pH 7.4) and fixed using 4% paraformaldehyde for 30 min. After that, 1 mL of 2 μg/mL DAPI was added and incubated for 5 min. The cellular uptake of various CFPE-labeled liposomes was then qualitatively observed *via* confocal laser scanning microscope (CLSM) (Leica, Germany). For quantitative uptake measurements, cells were incubated with CFPE-labeled liposomes for 4 h, detached by 0.25% trypsin, washed and resuspended in 0.5 mL PBS, and analyzed by flow cytometry.

2.6. Tumor spheroid uptake

The three-dimensional tumor spheroids of C26 were established as described previously[20,21] with some modification. Cells (2×10^3 per well) were plated onto a 96-well plate pre-coated with 40 μL 2% low melting point agarose. Several days later, spheroids (300–400 μm diameters) were treated with 0.3 mmol/L CFPE-labeled

R8-LP, PEG-LP and CL-R8-LP in the presence or absence of Cys (10 mmol/L) for 4 h. They were rinsed with PBS, followed by fixation of 4% paraformaldehyde for 0.5 h, and the spheroid fluorescent intensities captured by CLSM.

2.7. In vivo and ex vivo tumor imaging

In vivo and *ex vivo* fluorescence imaging experiments were performed using the Bio-Real *in vivo* imaging system (Quick View 3000, Bio-Real, AUSTRIA). The tumor-bearing mice were established by subcutaneous inoculation of 1×10^6 C26 cells in the left flank of BALB/c mice. The C26 tumor-bearing mice were randomly assigned into different groups with three mice each when the tumor diameters reached about 10 mm, and injected intravenously with DID-loaded liposomes at a dose of 500 μg DID/kg. Twenty-four hour after injection, mice were imaged with Bio-Real *in vivo* imaging system, and immediately euthanized with cervical dislocation. Hearts, livers, spleens, lungs, kidneys and tumors were collected. Organs were imaged with Bio-Real *in vivo* imaging system. DID fluorescence (excitation 644 nm, emission 665 nm) was monitored to localize the liposomes. For the qualitative evaluation of cellular uptake of the DID-loaded liposome in tumors, at 24 h post-injection, Cys (120 mg/kg) or PBS was injected. Tumors were excised and frozen sectioned 4 h later. Nuclei were stained with DAPI and fluorescent intensity of slices was observed *via* CLSM.

2.8. Statistics

Results were expressed as a mean ± standard deviation (SD). One-way ANOVA was used to compare differences, significance was defined as a P value of < 0.001.

3. Results

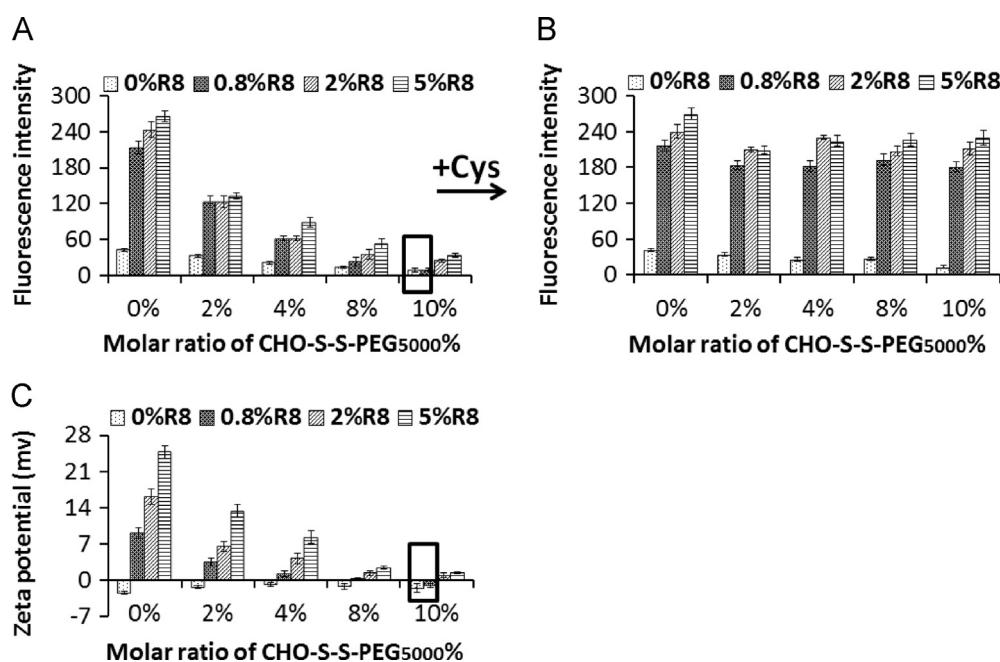### 3.1. Optimization of liposomal formulations

To develop the proposed co-modified liposomes, it should be noted that R8 were not functional in the presence of reduction-sensitive PEG. Then we evaluated the cellular uptake of different liposomes with various concentrations of CHO-S-S-PEG$_{5000}$ and R8. Cellular uptake of liposomes in the absence of Cys was significantly decreased with increasing the concentrations of CHO-S-S-PEG$_{5000}$ (Fig. 1A), which was correlated with their zeta-potentials (Fig. 1C). The addition of Cys produced a remarkable increase in the cellular uptake of liposomes modified with 0.8, 2, 5 mol% of R8 (Fig. 1B). The uptake and zeta potential of the 0.8 mol% R8+10 mol% CHO-S-S-PEG$_{5000}$ liposomal formulation was nearly the same as the control liposomal formulation (0 mol% R8+10 mol% CHO-S-S-PEG$_{5000}$), indicating this to be the optimal formulation, since R8 on the liposomal surface was complete masked by the aqueous layer of the PEG moiety.

3.2. Characterization of liposomes

After the optimal formulation was selected, the average diameter and zeta-potential of the CL-R8-LP and the control liposomes were determined (Table 1). Liposome sizes (diameter) were mainly around 90 nm. The zeta potential of R8-LP was strongly positive, whereas the CL-R8-LP and PEG-LP was nearly neutral.

3.3. Qualitative evaluation of cellular uptake in vitro

The cellular uptake of different liposomes (see Table 1) by C26 cells was investigated by CLSM. As shown in Fig. 2, R8-LP


Figure 1 Formulation optimization of liposomes modified with various concentrations of CHO-S-S-PEG$_{5000}$ and R8. The cellular uptake of different liposomes by C26 in the absence (A) and presence (B) of Cys. (C) The zeta potentials of different co-modified liposomes. The data represented the mean ± SD ($n=3$).

Table 1 Composition of different liposomes (mol%) and their characteristics.

| Abbreviation	Corresponding composition			Characteristic		
	EPC (%)	CHO (%)	Cholesterol anchored functional lipids	Size (nm)	PDI	Zeta (mV)
R8-LP	65.0	34.2	0.8% CHO-PEG$_{2000}$-R8	107.4$\pm$4.1	0.250$\pm$0.019	8.90$\pm$1.63
CL-R8-LP	65.0	24.2	0.8% CHO-PEG$_{2000}$-R8/10% CHO-S-S-PEG$_{5000}$	89.4$\pm$2.6	0.102$\pm$0.011	$-$1.17$\pm$0.38
PEG-LP	65.0	32.0	3% CHO-PEG$_{2000}$	96.3$\pm$5.4	0.148$\pm$0.021	$-$2.45$\pm$1.55

Data are mean$\pm$SD ($n=3$).
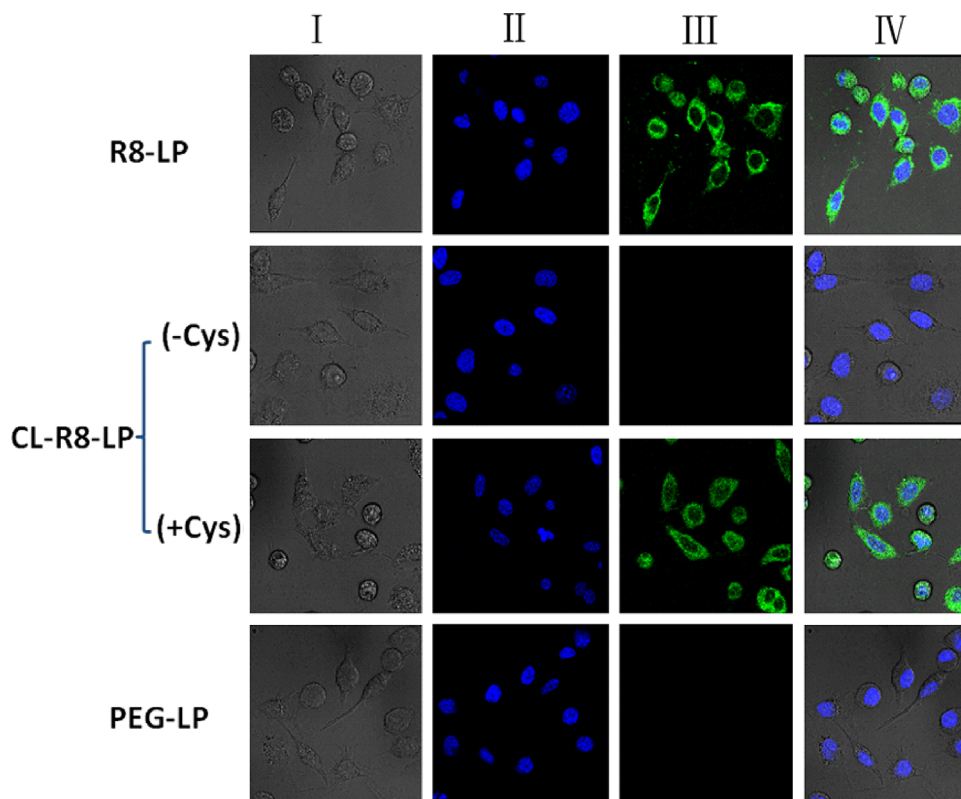
Figure 2 CLSM images of C26 cells incubated with different CFPE-labeled liposomes at 37 °C for 4 h. Left to right columns show: bright field (I), DAPI blue fluorescent nuclei (II), FITC-labeled green fluorescent liposomes (III), and merged fields (IV).

resulted in stronger fluorescence signals inside cells. Following the addition of 10 mol% of CHO-S-S-PEG$_{5000}$, the fluorescence signals of CL-R8-LP were almost invisible, indicating the function of R8 could be completely masked by CHO-S-S-PEG$_{5000}$. In the presence of Cys, however, the fluorescence intensity of CL-R8-LP was the same as R8-LP, suggesting CHO-S-S-PEG$_{5000}$ was detached from the surface of liposome in the reducing environment. The cellular uptake of PEG-LP without the modification of R8 was minimal.

3.4. Quantitative evaluation of cellular uptake in vitro

The quantitative results of cellular uptake were consistent with the results of fluorescence imaging. As shown in Fig. 3, the uptake amount of CL-R8-LP in the presence of Cys was 21.6 and 66.5 times higher than that of CL-R8-LP in the absence of Cys and
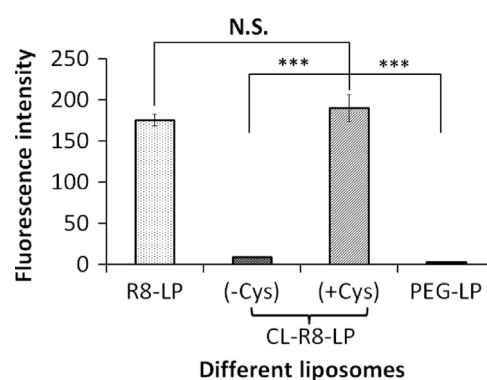
Figure 3 Fluorescence intensity of C26 cells measured by flow cytometer after incubated with different CFPE-labeled liposomes at 37 °C for 4 h. Data represent the mean$\pm$SD ($n=3$). ***$P<0.001$; N.S.=no significant difference.
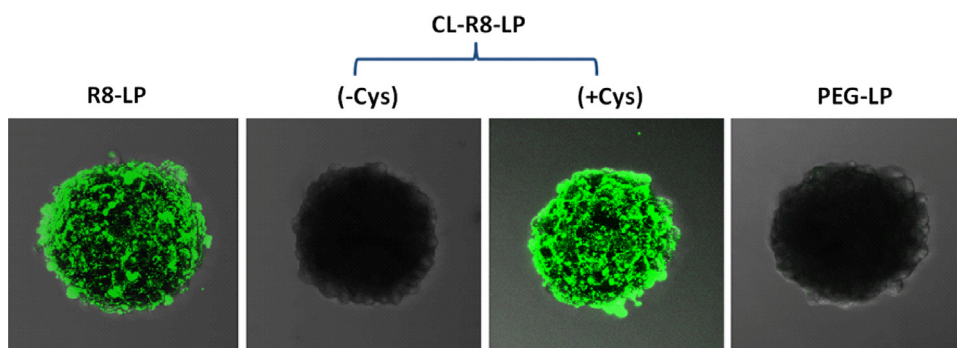
Figure 4 Representative CLSM images of C26 tumor spheroids incubated with different CFPE-labeled liposomes at 37 °C for 4 h.
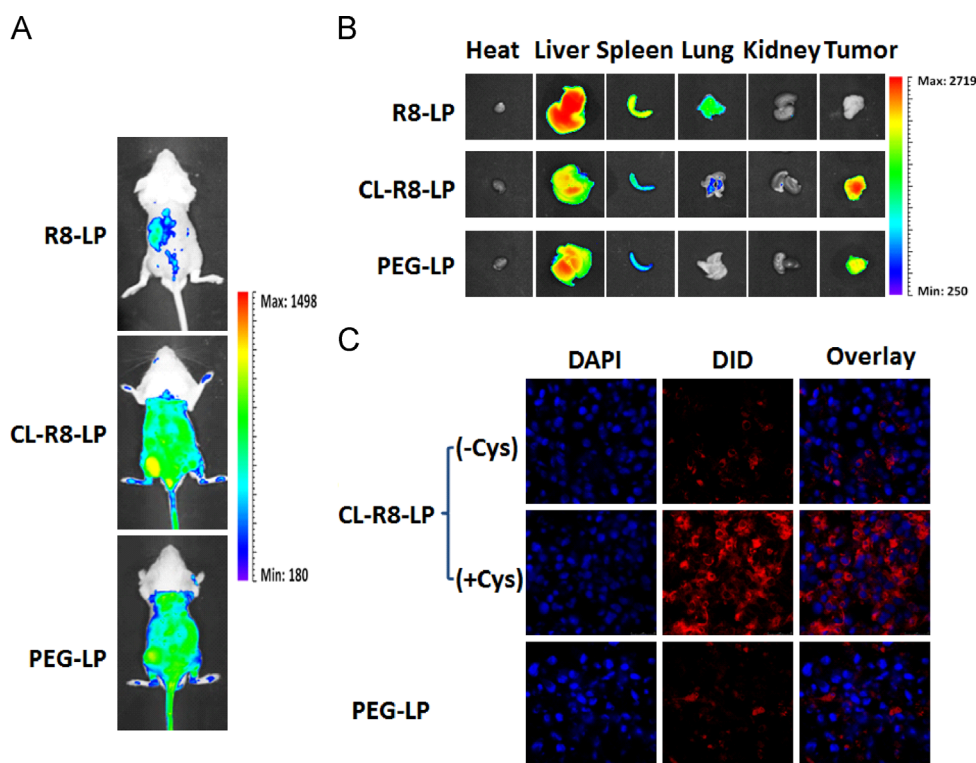

Figure 5 The representative *in vivo* (A) and *ex vivo* (B) images of C26 tumor-bearing mice 24 h after injection of DID-loaded liposomes. (C) The CLSM images of tumor frozen sections from C26 tumor-bearing mice receiving different DID-loaded liposomes.

PEG-LP respectively, and was comparable to the cellular uptake of R8-LP.

3.5. Evaluation of tumor spheroid uptake in vitro

The three-dimensional tumor spheroid models are commonly used as an ideal *in vitro* platform mimicking solid tumors to predict delivery efficiency and mechanism[22]. To further evaluate the delivery characteristics of liposomes, tumor spheroid uptake experiments were carried out. At 4 h, little fluorescence was detected within tumor spheroids from PEG-LP and CL-R8-LP (in the absence of Cys). In contrast, R8-LP and CL-R8-LP (in the presence of Cys) treated tumor spheroids demonstrated much greater fluorescence (Fig. 4), indicating that the modification and exposure of R8 on the liposomal surface could not only increase

the uptake by C26 cells but also facilitate the delivery of liposomes into tumor spheroids.

3.6. In vivo and ex vivo tumor imaging

To estimate the *in vivo* liposomal delivery to tumors, whole body optical imaging and *ex vivo* organ imaging were taken using the Bio-Real *in vivo* imaging system. Fig. 5A shows that 24 h after injection of different liposomes, fluorescence intensity in the tumors of CL-R8-LP-treated mice were significantly higher than that of R8-treated mice, and even slightly stronger than that of PEG-LP-treated mice. These findings were consistent with the results of *ex vivo* organ imaging at 24 h (Fig. 5B). In addition, R8-LP was mostly distributed in liver, spleen and lung, whereas CL-R8-LP and PEG-LP distributions in these organs were decreased significantly

(Fig. 5B). To further explore the delivery characteristics of CL-R8-LP and PEG-LP liposomes into cells after the sufficient tumor accumulation, tumor sections from C26 tumor-bearing mice receiving different liposomes were observed by CLSM. Fluorescence intensities in the tumor sections of CL-R8-LP (with Cys) treated mice were much higher than those of PEG-Lip and CL-R8-LP (without Cys) treated mice.

4. Discussion

For many years, CPPs have been widely applied in the drug delivery system for their excellent membrane-penetrating ability[23]. But the apparent ability of CPPs to penetrate virtually all cell types represents a major weakness for their *in vivo* use. To address this problem in the present study, the cholesterol anchored reduction-sensitive PEG synthesized by our laboratory was incorporated into CPP-modified liposomes. Compared with some other stimuli-sensitive materials, the cholesterol anchored reduction-sensitive PEG based on disulfide linkage has many advantages. First of all, cholesterol, serving as a neutral anchor, is inexpensive and more chemically stable than the most commonly used DSPE anchor[24]. Secondly, the disulfide linkage is easy to construct and is easily reduced[16]. Finally, the detachment of reduction-sensitive PEG is more controllable than pH-sensitive, MMP-sensitive or esterase-sensitive forms of PEG. Unlike the latter, which depend entirely on the specific physiological conditions, the former can be precisely cleaved by the exogenous reducing agent cysteine[19,25].

The objectives of the addition of sensitive PEG were to mask the nonspecific binding of CPPs in plasma, to increase the circulation time of carriers, and to enhance passive tumor targeting. Firstly, to maximize the masking effect of reduction-sensitive PEG on R8, we optimized the concentrations of CHO-S-S-PEG$_{5000}$ and R8, and the results (Fig. 1) clearly showed that the higher concentration of CHO-S-S-PEG$_{5000}$, the better the masking effect on R8. However, too high of a concentration of outer PEG layer would reduce the stability of the lipid bilayer[26]. In our lab, liposomes become unstable (indicated by large increases in PDI) when the concentrations of CHO-S-S-PEG$_{5000}$ exceed 10% (data not shown). By the modification of 10 mol% CHO-S-S-PEG$_{5000}$, the positive charge of R8 was completely shielded, and the zeta potential of co-modified liposome (CL-R8-LP) became neutral (Table 1), alleviating the electrostatic interaction between the positively charged CPPs and the negatively charged plasma membrane. Accordingly, the interaction between the positively charged CPPs and the negatively charged cell membrane weakened, and the uptake of CL-R8-LP by cells and tumor spheroids was much lower than that of R8-LP (Figs. 2–4). All these results suggest that the non-specificity of R8 shielded the outer PEG layer. And compared to the conventional non-cleavable PEG, the reduction-sensitive PEG modification couldn't bring about a steric hindrance that prevents carriers from efficient interaction with cellular membranes and/or endosomal membranes. This contradictory effect of PEGylation has been usually called the "PEG dilemma"[27,28]. As shown as Fig. 3, in the presence of Cys, the cellular uptake of CL-R8-LP was comparable to that of R8-LP, indicating the outer reduction-sensitive PEG layer was efficiently detached from the surface of liposomes, consistent with the qualitative results of cell uptake (Fig. 2) and tumor spheroid uptake (Fig. 4).

The results of *in vivo* and *ex vivo* tumor imaging (Fig. 5A and B) showed that R8-LP which lacks the PEG coating mainly distributed in RES related organs (liver, spleen and lung). Thus, CL-R8-LP can undergo a prolonged circulation time *in vivo* and benefit from the EPR effect, thereby achieving efficient accumulation within the tumor. It is worth noting that the tumor distributions of CL-R8-LP were also stronger than the conventional long circulation liposome PEG-LP. This can be explained by the conformational changes of outer PEG layer. Previous studies demonstrated that when the concentration of the outer PEG layer is relatively low ($<4\%$), PEG adopts a "mushroom" conformation. At increasingly higher concentrations, the "transition" and "brush" ($>8\%$) conformations emerge. The brush conformation has been linked to a "stealth" of carriers[26,29]. These results demonstrate that the modification with a relatively high concentration of reduction-sensitive PEG (10%) can help carriers to surmount efficiently the *in vivo* "kinetic barriers". Furthermore, after the sufficient tumor accumulations were achieved, this PEG coating will not affect the penetrating ability of liposomes into cells when the proper reducing environment is provided (Fig. 5C).

5. Conclusions

A cholesterol anchored reduction-sensitive PEG was applied here to help R8 modified liposomes achieve tumor targeted delivery *in vivo*. The combination of reduction-sensitive PEG and CPPs could overcome *in vivo* "kinetic barriers" and the cytoplasmic membrane barrier under the control of Cys. This new liposome formulation improves the non-specificity of CPPs and enhances the tumor targeted drug delivery of CPP-modified carriers.

Acknowledgments

References

1. Allen TM. Ligand-targeted therapeutics in anticancer therapy. *Nat Rev Cancer* 2002;**10**:750–63.
2. Byrne JD, Betancourt T, Brannon-Peppas L. Active targeting schemes for nanoparticle systems in cancer therapeutics. *Adv Drug Deliv Rev* 2008;**60**:1615–26.
3. Davis ME, Chen ZG, Shin DM. Nanoparticle therapeutics: an emerging treatment modality for cancer. *Nat Rev Drug Discov* 2008;**7**:771–82.
4. Torchilin V. Membrane barriers for bringing drugs inside cells and inside cell organelles. *J Membra Sci Technol* 2013;**3**:e114.
5. Snyder EL, Dowdy SF. Cell penetrating peptides in drug delivery. *Pharm Res* 2004;**21**:389–93.
6. Wadia JS, Dowdy SF. Transmembrane delivery of protein and peptide drugs by TAT-mediated transduction in the treatment of cancer. *Adv Drug Deliv Rev* 2005;**57**:579–96.
7. Futaki S, Hirose H, Nakase I. Arginine-rich peptides: methods of translocation through biological membranes. *Curr Pharm Des* 2013;**19**:2863–8.
8. Jin E, Zhang B, Sun X, Zhou Z, Ma X, Sun Q, et al. Acid active cell-penetrating peptides for *in vivo* tumor-targeted drug delivery. *J Am Chem Soc* 2013;**135**:933–40.
9. Frank MM. The reticuloendothelial system and bloodstream clearance. *J Lab Clin Med* 1993;**122**:487–8.
10. Tseng YC, Mozumdar S, Huang L. Lipid-based systemic delivery of siRNA. *Adv Drug Deliv Rev* 2009;**61**:721–31.

11. Vives E. Present and future of cell-penetrating peptide mediated delivery systems: "is the Trojan horse too wild to go only to Troy?" *J Control Release* 2005;**109**:77–85.

12. Sawant RM, Hurley JP, Salmaso S, Kale A, Tolcheva E, Levchenko TS, et al. "SMART" drugdelivery systems: double-targeted pH-responsive pharmaceutical nanocarriers. *Bioconjugate Chem* 2006;**17**:943–9.

13. Koshkaryev A, Sawant R, Deshpande M, Torchilin V. Immunoconjugates and long circulating systems: origins, current state of the art and future directions. *Adv Drug Deliv Rev* 2013;**65**:24–35.

14. Sawant R, Patel N, Torchilin V. Therapeutic delivery using cell-penetrating peptides. *Euro J Nanomed* 2013;**5**:141–58.

15. Koren E, Torchilin V. Cell-penetrating peptides: breaking through to the other side. *Trends Mol Med* 2012;**18**:385–93.

16. Kuai R, Yuan W, Qin Y, Chen H, Tang J, Yuan M, et al. Efficient delivery of payload into tumor cells in a controlled manner by TAT and thiolytic cleavable PEG co-modified liposomes. *Mol Pharm* 2010;**7**:1816–26.

17. Qin H, Tang J, Qin Y. A reduction-sensitive liposome based on the cholesterol derivatization for tumor targeting. 2012; ZL 201110197327.9.

18. Qin Y, Chen H, Yuan W, Kuai R, Zhang Q, Xie F, et al. Liposome formulated with TAT-modified cholesterol for enhancing the brain delivery. *Int J Pharm* 2011;**419**:85–95.

19. McNeeley KM, Karathanasis E, Annapragada AV, Bellamkonda RV. Masking and triggered unmaskingof targeting ligands on nanocarriers to improve drug delivery to brain tumors. *Biomaterials* 2009;**30**:3986–95.

20. Gao HL, Qian J, Yang Z, Pang ZQ, Xi ZJ, Cao SJ, et al. Whole-cell SELEX aptamer-functionalised poly(ethyleneglycol)-poly(ε-caprolactone) nanoparticles for enhanced targeted glioblastoma therapy. *Biomaterials* 2012;**33**:6264–72.

21. Perche F, Torchilin VP. Cancer cell spheroids as a model to evaluate chemotherapy protocols. *Cancer Biol Ther* 2012;**13**:1205–13.

22. Yao J, Zhang L, Zhou J, Liu H, Zhang Q. Efficient simultaneous tumor targeting delivery of all-trans retinoid acid and paclitaxel based on hyaluronic acid-based multifunctional nanocarrier. *Mol Pharm* 2013;**10**:1080–91.

23. Dietz GP, Bähr M. Delivery of bioactive molecules into the cell: the Trojan horse approach. *Mol Cell Neurosci* 2004;**27**:85–131.

24. Zhao XB, Muthusamy N, Byrd JC, Lee RJ. Cholesterol as a bilayer anchor for PEGylation and targeting ligand in folate-receptor-targeted liposomes. *J Pharm Sci* 2007;**96**:2424–35.

25. Kuai R, Yuan W, Li W, Qin Y, Tang J, Yuan M, et al. Targeted delivery of cargoes into a murine solid tumor by a cell-penetrating peptide and cleavable poly(ethylene glycol) comodified liposomal delivery system *via* systemic administration. *Mol Pharm* 2011;**8**:2151–61.

26. Li SD, Huang L. Nanoparticles evading the reticuloendothelial system: role of the supported bilayer. *Biochim Biophys Acta* 2009;**1788**:2259–66.

27. Hatakeyama H, Akita H, Harashima H. A multifunctional envelope type nano device (MEND) for gene delivery to tumours based on the EPR effect: a strategy for overcoming the PEG dilemma. *Adv Drug Deliv Rev* 2011;**63**:152–60.

28. Wang T, Upponi JR, Torchilin VP. Design of multifunctional non-viral gene vectors to overcome physiological barriers: dilemmas and strategies. *Int J Pharm* 2012;**427**:3–20.

29. Garbuzenko O, Barenholz Y, Priev A. Effect of grafted PEG on liposome size and on compressibility and packing of lipid bilayer. *Chem Phys Lipids* 2005;**135**:117–29.